EUROPEAN ORGANIZATION FOR NUCLEAR RESEARCH

**Proposal to the ISOLDE and Neutron Time-of-Flight Committee**

# Laser spectroscopic studies along the Al isotopic chain and the isomer-shift of the self-conjugate $^{26}$Al nucleus

January 11, 2016

H. Heylen[1], S. Malbrunot-Ettenauer[2], M.L. Bissell[3], K. Blaum[4], B. Cheal[5], L. Filippin[6], R.F. Garcia Ruiz[3], W. Gins[1], M. Godefroid[6], C. Gorges[7], S. Kaufmann[7], Á. Koszorús[1], J. Krämer[7], M. Kowalska[2], G. Neyens[1], R. Neugart[4,8], W. Nörtershäuser[7], R. Sánchez[9], Z.Y. Xu[1], X.F. Yang[1], D.T. Yordanov[10].

[1] *KU Leuven, Instituut voor Kern- en Stralingsfysica, 3001 Leuven, Belgium*
[2] *Experimental Physics Department, CERN, CH-1211 Geneva 23, Switzerland*
[3] *School of Physics and Astronomy, The University of Manchester, Manchester, M13 9PL, UK*
[4] *Max-Plank-Institut für Kernphysik, D-69117 Heidelberg, Germany*
[5] *Oliver Lodge Laboratory, Oxford Street, University of Liverpool, L69 7ZE, United Kingdom*
[6] *Université libre de Bruxelles, B 1050 Brussels, Belgium*
[7] *Institut für Kernphysik, TU Darmstadt, D-64289 Darmstadt, Germany*
[8] *Institut für Kernchemie, Universität Mainz, D-55128 Mainz, Germany*
[9] *GSI Helmholtzzentrum für Schwerionenforschung, D-64291 Darmstadt, Germany*
[10] *Institut de Physique Nucléaire Orsay, IN2P3/CNRS, 91405 Orsay Cedex, France*

**Spokespersons:** Stephan Malbrunot-Ettenauer, stephan.ettenauer@cern.ch, Hanne Heylen, hanne.heylen@fys.kuleuven.be
**Contact person:** Stephan Malbrunot-Ettenauer, stephan.ettenauer@cern.ch

**Abstract:** We propose to measure the isomer shift in the self-conjugate $^{26}$Al ($N = Z = 13$) nucleus along with the isotope shifts of $^{24-33}$Al using bunched-beam collinear laser spectroscopy at the COLLAPS beam line at ISOLDE. These isomer and isotope shifts allow the extraction of precise mean-square charge radii, in particular the difference in charge radius between the $I = 5^+,\ T = 0$ ground state and $I = 0^+,\ T = 1$ isomer in $^{26}$Al. This charge radius difference, in comparison with the odd-even staggering in the Al-chain, is an excellent probe to study proton-neutron pairing correlations, as was previously illustrated for $^{38}_{19}$K$_{19}$ [1]. Furthermore, accurate knowledge of the mean-square charge radius in $^{26m}$Al is essential to reliably calculate its isospin-symmetry breaking correction which is important to extract the CKM matrix element $V_{\rm ud}$ from the $0^+ \rightarrow 0^+$ superallowed $\beta$-decay data. Finally, the charge radii of the neutron-rich Al isotopes will probe the development of deformation at the border of the island of inversion.

**Requested shifts:** 21 shifts (split into 2 runs over 1 year)

# 1 Motivation

The mean-square charge radius is a fundamental property of the atomic nucleus as it contains information on the nuclear size and shape. Notably the charge radii of self-conjugate nuclei, having an equal number of protons and neutrons, are of considerable interest for nuclear pairing studies as well in the search for physics beyond the standard model. Here we propose a direct measurement of the isomer shift in $^{26}$Al ($N = Z = 13$), yielding the difference in mean-square charge radius between the $I = 5^+$ ground state and $I = 0^+$ isomer. Additionally, the mean-square charge radii and their odd-even staggering in the Al isotopic chain will be determined by measuring the isotope shifts of $^{24-33}\mathrm{Al}_{11-19}$. These measurements are an important probe for neutron-proton pairing and provide an accurate charge radius of $^{26m}$Al, which is a crucial input parameter for the determination of the isospin-symmetry-breaking corrections in superallowed $\beta$ decays. Extending the knowledge in experimental charge radii to the Al isotopes will further give insight in the evolution of nuclear structure in and beyond the neutron *sd* shell. All these science motivations will be discussed separately.

## 1.1 Proton-neutron pairing

Similar to Cooper pairs in electronic systems, protons and neutrons in a nucleus can couple to form correlated pairs. The occurrence of such nuclear pairs is a basic feature of our understanding of the nuclear structure, for example to explain the difference in binding energies between even-even nuclei and their odd neighbours. Whereas the importance of proton-proton (*pp*) and neutron-neutron (*nn*) pairing has long since been recognized, proton-neutron (*pn*) pairing is still an active research area [2]. Notably, the role of isovector ($T = 1$) and isoscalar ($T = 0$) pairing correlations is of interest.
Proton-neutron pairing is most suitably studied in nuclei near the $N = Z$ line where protons and neutrons occupy the same orbitals, enhancing the correlations between them. Most of the experimental information on *pn* pairing comes from the study of the binding energies, where in particular the relation of *pn* pairing and the Wigner energy term is debated [3, 4]. Moreover, *pn* pair transfer reactions are a promising tool because of the significant cross-section enhancement of deuteron-like transfer in case a nuclear state is dominated by *pn* correlations [5, 6]. Competition between $T = 0$ and $T = 1$ states is further investigated in the low-energy spectrum of odd-odd self-conjugate nuclei. Apart from $^{58}$Cu and $^{34}$Cl, self-conjugate nuclei with mass $A > 40$ have $T = 1$ ground states while in $A < 40$ an isospin inversion is seen resulting in $T = 0$ ground states. Initially this was seen as an indication for an increased importance of isoscalar pair correlations in light isotopes but more recently it has been shown that these observations can also be explained by the interplay between isovector pair correlation energy and the symmetry energy [2]. A detailed understanding of the competing $T = 0$ and $T = 1$ contributions to the nuclear symmetry energy requires the systematic investigation of the $T$ =1 *pn* pairing correlation.

Recently, also the difference in size between the $T = 0$ and $T = 1$ states has shown to be an excellent probe for proton-neutron pairing [1]. The mean-square charge radius

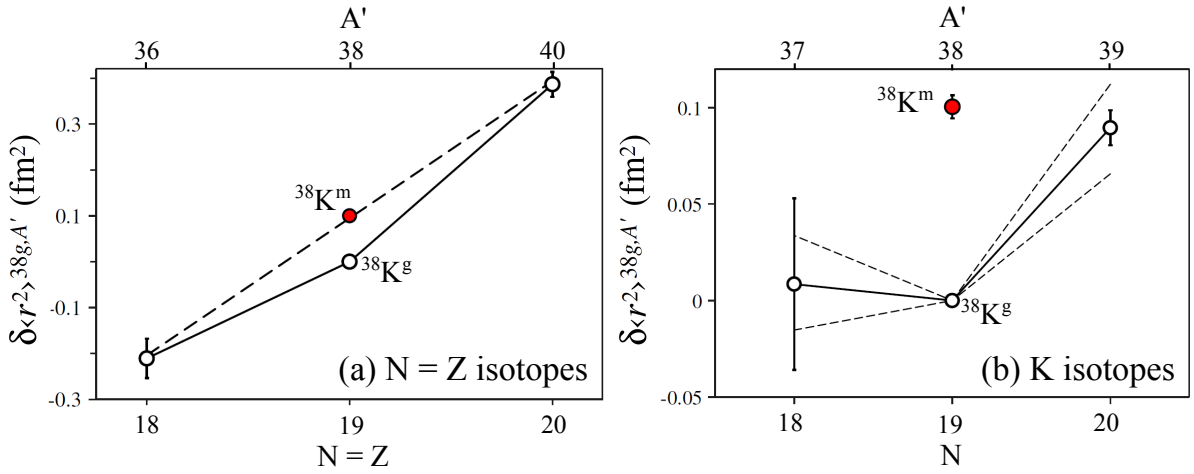


Figure 1: (a) Mean-square charge radii of the $T = 0$ ground state and $T = 1$ isomer of $^{38}$K compared to the $T = 1$ ground state radii of the neighbouring $^{36}_{18}\mathrm{Ar}_{18}$ and $^{40}_{20}\mathrm{Ca}_{20}$ nuclei. (b) Difference in mean-square charge radius of the $^{38}$K ground state and isomer compared to the odd-even staggering in the neighbouring K isotopes. Both figures are taken from [1].

difference $\delta\langle r^2\rangle^{g,m}$ between the $I = 3^+,\ T = 0$ ground state and $I = 0^+, T = 1$ isomer in $^{38}$K ($N = Z = 19$) was obtained via a precise isomer shift measurement using collinear laser spectroscopy at COLLAPS. To explain the larger mean-square charge radius of the $T = 1$ isomer compared to the $T = 0$ ground state, an intuitive interpretation in terms of *pn* pairing was put forward, similar to the explanation of normal odd-even staggering in terms of *pp* and *nn* pairs. The consistently larger mean-square charge radius in even $N$ (or $Z$) nuclei as compared to their odd (or odd-odd) neighbours is generally understood as due to scattering of *nn* or *pp* pairs to less bound, i.e. spatially more extended, orbitals while in odd(-odd) nuclei this scattering is blocked by addition of an odd proton or neutron. Because of the charge independence of the nuclear force, $T = 1$ *pn*-pairs should be treated on equal footing as the *pp* and *nn* counterparts[1] and pair scattering of the isovector *pn*-pair therefore leads to a larger charge radius of the $T = 1$ isomer in $^{38}$K. Indeed, as shown in Fig. 1(a), the isomer lies nicely on the $N = Z$ line established by the $T = 1$ ground states in the even-even neighbors, while the $T = 0$ $^{38}$K ground state is smaller due to the blocking of pair scattering. Likewise, the difference in charge radius between ground state and isomer is larger than the normal odd-even scattering because the blocking by the odd proton in the K isotopes, is removed for the $T = 1$ isomer in $^{38}$K due to *pn*-pair scattering, illustrated in Fig. 1(b). The role of *pn* pairing was further investigated by large-scale shell-model calculations using the modified ZBM2 interaction, which supported the conclusions above.

So far the difference in mean-square charge radius between the ground state and isomer is only known in 2 other self-conjugate nuclei: $^{50}_{25}\mathrm{Mn}_{25}$ [7] and $^{42}_{21}\mathrm{Sc}_{21}$ [8]. When taking into account a different sign due to the isospin inversion above $A > 40$, the measured value for $^{50}$Mn is almost identical to $^{38}$K, while the value of $^{42}$Sc is more than twice as large.

[1]Due to the Pauli principle like-nucleons can only couple to $T = 1$ pairs.

At the moment, this apparent mass dependence of $\delta\langle r^2\rangle^{g,m}$ is not understood. Although shell-model calculations using the modified ZBM2 interaction were reasonably successful at predicting $\delta\langle r^2\rangle^{g,m}$ in $^{38}$K, they predict only a moderate increase in $\delta\langle r^2\rangle^{g,m}$ for $^{42}$Sc, at variance with the experimental observations. It is also a priori not clear whether such shell-model calculations can be generalized to other mass regions in a straightforward way. Hence, more experimental input is essential to shed light on these issues and to provide a more global picture on the size of the phenomenon in different self-conjugate nuclides. As such, the $N = Z = 13$ nucleus $^{26}$Al provides an excellent candidate for the next measurement to benchmark *pn*-pairing in self-conjugate nuclides, especially as it represents the lightest case with a long-lived $T = 1$ isomer. Measurements of the mean-square charge radii of $^{24-33}\mathrm{Al}_{11-19}$ will further allow the determination of the odd-even staggering in the Al-chain. As illustrated for $^{38}$K in Fig. 1(b), this information is essential to thoroughly test the proposed interpretation in terms of *pn*-pairing.

## 1.2 Superallowed $\beta$ decays, $V_{\mathrm{ud}}$, and the charge radius of $^{26m}$Al

Superallowed $0^+ \rightarrow 0^+$ $\beta$ decays remain the preferred way to access $V_{\mathrm{ud}}$ of the Cabibbo-Kobayashi-Maskawa (CKM) quark mixing matrix [9]. Combined with the other matrix elements of the top row, it establishes the most demanding unitarity test in the CKM matrix, $|V_{\mathrm{ud}}|^2 + |V_{\mathrm{us}}|^2 + |V_{\mathrm{ub}}|^2 = 1$ which poses stringent limits on physics beyond the Standard Model of particle physics [9]. Recently, the uncertainty contribution of $|V_{\mathrm{us}}|$ to the test was reduced by lattice QCD calculations [10, 11, 12], which now demands further progress on $V_{\mathrm{ud}}$ and to scrutinize its associated uncertainties.

Among the 14 cases considered in the determination of $V_{\mathrm{ud}}$ from superallowed $\beta$ decays, $^{26m}$Al carries special weight as its superb precision rivals all other cases combined. This is illustrated in Fig. 2 which shows the fractional uncertainties to the corrected $\mathcal{F}t$ values, the quantity to determine $V_{\mathrm{ud}}$, for the lighter and more precisely known superallowed $\beta$ emitters. The dominating uncertainty in $^{26m}$Al (and in most other cases) is not due to experiment but is found in theoretical corrections which take into account that isospin symmetry is slightly broken. Within the shell model, these isospin-symmetry-breaking (ISB) corrections, $\delta_C$, are separated into two parts, $\delta_C = \delta_{C1} + \delta_{C2}$, where $\delta_{C1}$ reflects configuration mixing within the restricted shell model space and $\delta_{C2}$ represents the radial overlap correction. The latter is generally larger in value, for instance, in $^{26m}$Al the ISB corrections account for $\delta_{C1} = 0.030(10)$ % and $\delta_{C2} = 0.280(15)$ % when considering Saxon-Woods radial functions for the determination of $\delta_{C2}$ [13]. In these calculations, the Saxon-Woods potential is constructed utilizing the nuclear charge radius of the superallowed $\beta$ emitter as an input parameter. However, the charge radius of superallowed $\beta$ emitters is in many cases not known experimentally. For the determination of $\delta_{C2}$ with Saxon-Woods radial functions, the charge radius is then extrapolated from stable isotopes and the associated uncertainties are generously inflated to account for the lack in experimental data [13, 14]. Consequently, uncertainties in charge radii enter into the error estimate of $\delta_{C2}$ and are a significant contribution to the uncertainty of $\delta_{C2}$. Indeed, when an updated compilation of experimental charge radii [15] was considered in the latest survey of superallowed $\beta$ decays [9], the value of $\delta_{C2}$ was noticeably shifted (although within previously quoted uncertainties) for all three superallowed $\beta$ emitters with a new

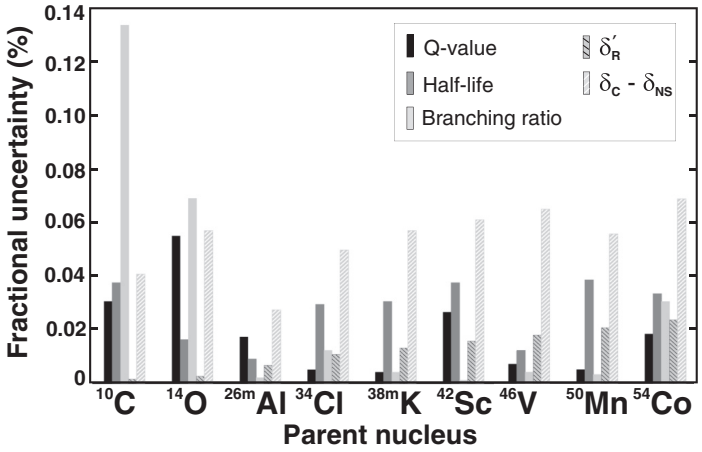


Figure 2: Fractional uncertainties to the corrected $\mathcal{F}t$ values of the lighter superallowed $\beta$ emitters. Figure from [9].

charge radius. In addition, $^{74}$Rb's charge radius determined in recent laser-spectroscopic work lead to a reduction of the uncertainty on $\delta_{C2}$ by 20 % [16].
$^{26m}$Al is among those cases without a measurement of its nuclear charge radius. The outstanding situation found in $^{26m}$Al as the most precisely studied superallowed $\beta$ emitter, comparable in precision to all other cases combined, calls for an experimental determination of its nuclear charge radius. Currently, the size of the uncertainty in $\delta_{C2}$ due to the extrapolation to $^{26m}$Al's charge radius is about one third of the uncertainty in $\delta_{C2}$ (compare [14] and [13]). Our proposed measurement will effectively eliminate the charge radius as a source of uncertainty in the isospin-symmetry-breaking corrections $\delta_C$ of $^{26m}$Al. Most importantly, an actual measurement will place $^{26m}$Al's charge radius as used in the Saxon-Woods radial functions and hence its $\delta_C$ on solid experimental grounds which we consider as vital and adequate given the level of precision and accuracy achieved in studies of fundamental symmetries with superallowed $\beta$ decays.

## 1.3 Nuclear charge radii to probe evolution of nuclear structure

Due to their sensitivity to the size and shape of a nucleus, systematic measurements of nuclear charge radii along isotopic chains have provided important signatures for the evolution of nuclear structure all across the nuclear chart. However, as shown on Fig. 3, between Mg ($Z = 12$) and Ar ($Z = 18$) the charge radii are known experimentally only for stabile nuclides. Hence, the proposed measurements of the mean-square charge radii of $^{24,33}$Al$_{11,20}$ isotopes will be a first step to fill this gap.
While in the heavy mass regions the charge radii generally vary smoothly with $Z$ and $N$, in the light and medium mass nuclei this is no longer the case due to the rapid change and rich variety in nuclear structure. For example, in the Ne ($Z = 10$) isotopes the charge radii highlight effects of a proton-halo nucleus, clustered configurations, classical shell gaps, new subshell gaps and deformation within the mere range of 12 neutron numbers between $N = 7$ to $N = 18$ [21]. Towards $N = 20$ there is a marked onset of deformation

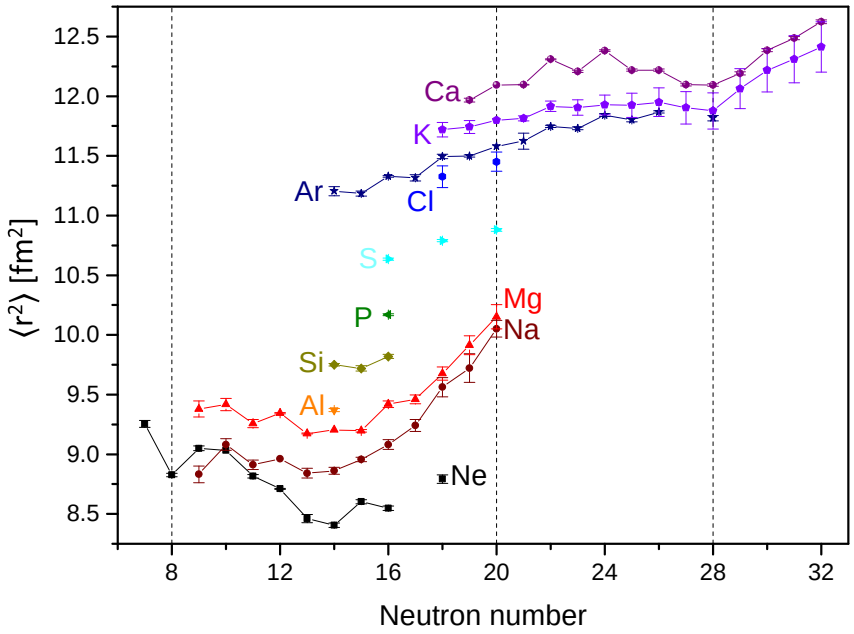


Figure 3: The experimentally mean-square charge radii $\langle r^2 \rangle$ between Ne ($Z = 10$) and Ca (Z=10), data taken from [17, 18, 19, 20]

in the so-called island of inversion, clearly seen in the increase in the charge radii of the Na ($Z = 11$) and Mg ($Z = 12$) isotopes [18], confirming the observations from measured moments that the $^{31,33}$Mg and $^{30,31}$Na have intruder ground state structures [22, 23]. Measuring the Al charge radii will therefore be important to further characterise the nuclear structure in this region. Similar to Ne and Mg, clustering effects might play a role for the neutron-deficient Al isotopes. The neutron-rich Al isotopes around $N = 20$ on the other hand are known to lie on the border of the island of inversion between the spherical Si and deformed Mg nuclei. The transitional character of Al was already studied in $g$-factor and quadrupole moment measurements which have shown a significant amount of intruder admixtures in the ground state of the neutron-rich $^{33,34}$Al isotopes [24, 25, 26]. As the quadrupole moment of $^{33}$Al is of the same size as that of $^{31}$Al, it was argued however that these intruder configurations are not associated with an increase in static deformation. Contrary to quadrupole moments, mean-square charge radii are also sensitive to dynamical deformation and hence the charge radius of $^{33}$Al will provide an essential and complementary piece of information to study the development of deformation in the island of inversion.

# 2 Experimental method

For the proposed measurements, standard methods of collinear laser spectroscopy of bunched beams will be followed as they are routinely being employed at COLLAPS (e.g. [1]). These measurements will reveal the hyperfine structures of the studied Al isotopes yielding hyperfine parameters and isotope shifts $\delta\nu^{A,A'}$. From the latter, changes

in mean-square charge radii $\delta\langle r^2\rangle$ are extracted according to

$$\delta\nu^{A,A'} = M\frac{A'-A}{A\cdot A'} + F\delta\langle r^2\rangle^{A,A'}, \quad (1)$$

where $M$ and $F$ are mass and field shift factor, respectively. For $^{26g,26m}$Al, collinear laser spectroscopy allows the direct measurements of the isomer shift since the hyperfine structure centroids for both the ground state and the isomer can be determined in a single hyperfine spectrum. The advantage of this direct determination was clearly demonstrated for $^{38}$K [1] where a previous indirect determination of the isomer shift by the combination of two data sets, led to large error bars and as a consequence, to the wrong conclusion on the relative size of the ground state and isomer.

Due to a lack of suitable transitions in Al ions, spectroscopy is performed on atoms which are formed when Al ions delivered by ISOLDE are neutralized in COLLAPS' charge exchange cell which is filled with Na vapour. Based upon our previous work (IS457) on Ga atoms, which have very similar structure and transitions, we expect that the two states of the $^2P^o$ doublet are populated roughly equally in the charge exchange. Several strong transitions can be considered (compare also with Fig. 4a). We exclude the transitions to the $^2D$ doublet at 308 nm and 309 nm, respectively, since the two $^2D$ states are very close in energy ($\Delta E \approx 0.2$ meV) resulting in mixing of the two transitions [27]. This could lead to anomalies in the optical isotope shifts in analogy to what has been observed in Sm isotopes [28]. Such complications are naturally avoided in the transitions to the $^2S_{1/2}$ singlet at 396 nm and 394 nm, respectively. Due to the finite probability density of the s-electron at the nuclear site, these transitions are also more sensitive to the nuclear charge radius. The $^2P^o_{3/2} \rightarrow {}^2S_{1/2}$ transition with an Einstein coefficient of $A = 1.0\cdot 10^8$/s is stronger than $^2P^o_{1/2} \rightarrow {}^2S_{1/2}$ ($A = 5.1\cdot 10^7$/s). Moreover, it is also sensitive to the quadrupole moments of the investigated Al isotopes (not known for $^{24,29,30}$Al) and is hence the preferred transition. Laser light at this wavelength can be produced by frequency doubling 792 nm provided by a Ti:Sa laser.

As mentioned before, the transition dependent mass and field shift $M$ and $F$ are required to extract the changes in the mean-square charge radii $\delta\langle r^2\rangle^{A,A'}$ from the measured isotope shift. Corresponding atomic-physics calculations of $M$ and $F$ for the $^2P^o_{3/2} \rightarrow {}^2S_{1/2}$ transition are currently underway [29]. Finally, the charge radii of the studied Al isotopes can be determined by comparing $\delta\langle r^2\rangle^{A,A'}$ to the root-mean-square charge radius of $^{27}$Al [15], which is known from muonic-atom and electron-scattering measurements.

# 3 Beam time request

Following our science motivation, we request ISOLDE beams of $^{24-33}$Al (see Tab. 1). $^{27}$Al will serve as the reference throughout the entire measurement. Two shifts of stable $^{27}$Al beam are requested for setup and confirmation of the spectroscopic scheme prior to the measurements of radioactive nuclides. Operation and use of HRS and the cooler and buncher ISCOOL will be required from the beginning. Moreover, RILIS will be essential to increase the yields of the Al isotopes.

To date, all yields for Al isotopes (see Fig. 4b) listed in the ISOLDE yield database as well

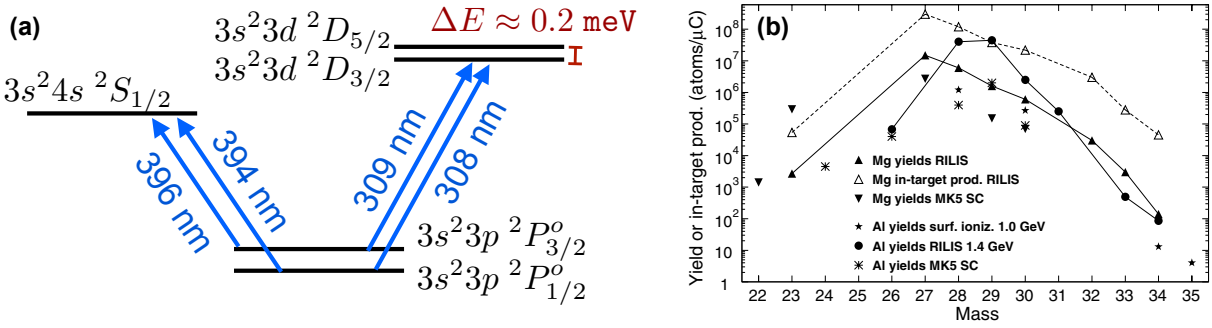


Figure 4:
**(a)** Simplified level scheme and relevant atomic transitions in Al atoms.
**(b)** ISOLDE yields of Al isotopes. At $A = 26$, the displayed yields are for $^{26m}$Al. Figure from [30].

as with ISOLDE coupled to the PSB are based on UCx targets. While lighter targets such as a SiC target may result to higher yields of $^{26,26m}$Al, the reported yields obtained by a UCx target are sufficient for our proposed measurements. However, for $^{24}$Al, where yields were only measured at ISOLDE-SC, the ISOLDE-PSB yield from UCx targets could be lower than at ISOLDE-SC because of its potentially lower production cross section at the higher proton energy [31]. We hence request a test for $^{24}$Al's yield on the UCx target to establish the yield at the end of our first beamtime which will focus on the neutron-rich Al isotopes. Based on these results, a second run may benefit from a lighter target and/or the use of LIST for suppression of Na contamination in the beams of lighter Al isotopes. Due to the similarity of the spectroscopy scheme and experimental setup, the shift request is based on our previous experience with Ga atoms (IS457): We request 1 shift per nuclide with higher yields ($> 10^6$ ions/$\mu$C) and 2 shifts per nuclides with lower yields. Taking into account the expected lower yield of a few thousand ions per $\mu$C for $^{24,33}$Al [31], 4 shifts will be required for the measurement of each of these nuclides. An overview over the Al isotopes and the requested shifts is provided in Tab. 1.
**Summary of requested shifts:** 21 shifts (2 for setup and 19 for online measurements of $^{24-33}$Al split into two separate beamtimes).

# References


[1] M. L. Bissell, et al. Proton-Neutron Pairing Correlations in the Self-Conjugate Nucleus $^{38}$K Probed via a Direct Measurement of the Isomer Shift. *Phys. Rev. Lett.*, 113:052502, Jul 2014.

[2] S. Frauendorf, et al. Overview of neutron-proton pairing. *Progress in Particle and Nuclear Physics*, 78:24 – 90, 2014.

[3] K. Neergård. Pairing theory of the symmetry energy. *Phys. Rev. C*, 80:044313, 2009.

Table 1: List of Al isotopes to be studied in this proposal. Each nuclide is listed with half-life, magnetic moment $\mu$, electric quadrupole moment $Q$, yields at ISOLDE, and the requested shifts. All yields are based on UCx targets and RILIS as listed in the ISOLDE yield database. $\mu$ and $Q$ from [32].

| nuclide | spin$^{\text{parity}}$ | half-life | $\mu$ [$\mu_N$] | Q [b] | yield [ions/$\mu$C] | shifts (target) |
|---|---|---|---|---|---|---|
| $^{24}$Al | $4^+$ | 2.1 s | 2.99(9) | ? | 4.5E+03 [a] | 4* |
| $^{25}$Al | $5/2^+$ | 7.2 s | 3.6455(12) | 0.24(2) | not listed | 2 |
| $^{26}$Al | $5^+$ | 7.2E+5 y | 2.804(4) | 0.27(3) | not listed | 2 |
| $^{26m}$Al | $0^+$ | 6.3 s | - | - | 6.8E+04 | 2 |
| $^{27}$Al | $5/2^+$ | stable | 3.6415069(7) | 0.1466 | | |
| $^{28}$Al | $3^+$ | 2.2 min | 3.242(5) | 0.175(14) | 4.0E+07 | 1 |
| $^{29}$Al | $5/2^+$ | 6.6 min | ? | ? | 4.5E+07 | 1 |
| $^{30}$Al | $3^+$ | 3.6 s | 3.010(7) | ? | 2.5E+06 | 1 |
| $^{31}$Al | $5/2^+$ | 640 ms | 3.830(5) | 0.1340(16) | 2.5E+05 | 2 |
| $^{32}$Al | $1^+$ | 33 ms | 1.959(9) | 0.024(2) | not listed | 2 |
| $^{33}$Al | $5/2^+$ | 42 ms | 4.088(5) | 0.132(16) | 1 - 4E4 [b] | 4 |

[a] Yield measured at ISOLDE-SC with a UCx target; see text for details

[b] Estimate based on recent yield measurements on $^{34}$Al [31], which are not listed in the yield database.


[4] I. Bentley, et al. Relation between Wigner energy and proton-neutron pairing. *Phys. Rev. C*, 88:014322, 2013.

[5] P. Fröbrich. Enhancement of deuteron transfer reactions by neutron-proton pairing correlations. *Physics Letters B*, 37(4):338 – 340, 1971.

[6] A.O. Macchiavelli, et al. The 56Ni(3He,p) Reaction and the Question of T = 0, T = 1 Pairing in N = Z Nuclei. *ANL Physics Division Annual Report*, page 21, 2002.

[7] F.C. Charlwood, et al. Ground state properties of manganese isotopes across the shell closure. *Physics Letters B*, 690(4):346 – 351, 2010.

[8] B. Cheal. private communication.

[9] J. C. Hardy, et al. Superallowed $0^+ \to 0^+$ nuclear $\beta$ decays: 2014 critical survey, with precise results for $V_{ud}$ and CKM unitarity. *Phys. Rev. C*, 91:025501, 2015.

[10] R. J. Dowdall, et al. $V_{us}$ from $\pi$ and $K$ decay constants in full lattice QCD with physical $u$, $d$, $s$, and $c$ quarks. *Phys. Rev. D*, 88:074504, 2013.

[11] A. Bazavov, et al. Determination of $|V_{us}|$ from a Lattice QCD Calculation of the $K \to \pi\ell\nu$ Semileptonic Form Factor with Physical Quark Masses. *Phys. Rev. Lett.*, 112:112001, 2014.

[12] A. Bazavov, et al. Charmed and light pseudoscalar meson decay constants from four-flavor lattice QCD with physical light quarks. *Phys. Rev. D*, 90:074509, 2014.

[13] I. S. Towner, et al. Improved calculation of the isospin-symmetry-breaking corrections to superallowed Fermi $\beta$ decay. *Phys. Rev. C*, 77:025501, 2008.

[14] I. S. Towner, et al. Calculated corrections to superallowed Fermi $\beta$ decay: New evaluation of the nuclear-structure-dependent terms. *Phys. Rev. C*, 66:035501, 2002.

[15] I. Angeli. A consistent set of nuclear rms charge radii: properties of the radius surface R(N,Z). *Atomic Data and Nuclear Data Tables*, 87(2):185 – 206, 2004.

[16] E. Mané, et al. First Experimental Determination of the Charge Radius of $^{74}$Rb and Its Application in Tests of the Unitarity of the Cabibbo-Kobayashi-Maskawa Matrix. *Phys. Rev. Lett.*, 107:212502, 2011.

[17] I. Angeli et al. Table of experimental nuclear ground state charge radii: An update. *Atomic Data and Nuclear Data Tables*, 99(1):69 – 95, 2013.

[18] D. T. Yordanov, et al. Nuclear Charge Radii of $^{21\text{-}32}$Mg. *Phys. Rev. Lett.*, 108:042504, 2012.

[19] K. Kreim, et al. Nuclear charge radii of potassium isotopes beyond. *Phys. Lett. B*, 731(0):97 – 102, 2014.

[20] R.F. Garcia-Ruiz. *Collinear Laser Spectroscopy on exotic Ca Isotopes towards new magic numbers $N = 32$ and $N = 34$.* PhD thesis, KULeuven, 2015.

[21] K. Marinova, et al. Charge radii of neon isotopes across the *sd* neutron shell. *Phys. Rev. C*, 84:034313, 2011.

[22] Gerda Neyens. Multiparticle-multihole states in $^{31}$Mg and $^{33}$Mg: A critical evaluation. *Phys. Rev. C*, 84:064310, 2011.

[23] *Proceedings of the Second International Conference on Exotic Nuclei and Atomic Masses*. AIP Conf. Proc. No. 455 (AIP, New York, 1999) Bellaire, Michigan, 1998.

[24] P. Himpe, et al. g factors of $^{31,32,33}$Al: Indication for intruder configurations in the 33Al ground state. *Physics Letters B*, 643(5):257 – 262, 2006.

[25] P. Himpe, et al. g factor of the exotic isotope $^{34}$Al: probing the and shell gaps at the border of the island of inversion. *Physics Letters B*, 658(5):203 – 208, 2008.

[26] K. Shimada, et al. Erosion of shell in investigated through the ground-state electric quadrupole moment. *Physics Letters B*, 714(25):246 – 250, 2012.

[27] T. G. Cooper, et al. The nuclear magnetic moment of $^{26}$Al by atomic beam laser spectroscopy. *Journal of Physics G: Nuclear and Particle Physics*, 22(1):99, 1996.

[28] J. A. R. Griffith, et al. Anomalies in the optical isotope shifts of samarium. *Journal of Physics B: Atomic and Molecular Physics*, 14(16):2769, 1981.

[29] Livio Filippin. Accounting for core-core effects in multiconfguration calculations of isotope shifts. Talk at the ECT* Workshop "The interplay between atomic and nuclear physics to study exotic nuclei", 2015.

[30] U. Köster, et al. On-line yields obtained with the ISOLDE RILIS. *Nuclear Instruments and Methods in Physics Research Section B: Beam Interactions with Materials and Atoms*, 204:347 – 352, 2003. 14th International Conference on Electromagnetic Isotope Separators and Techniques Related to their Applications.

[31] Joao Pedro Ramos and Thierry Stora, private communications, 2016.

[32] N.J. Stone. TABLE OF NUCLEAR MAGNETIC DIPOLE AND ELECTRIC QUADRUPOLE MOMENTS. *NDC(NDS)-0658, INDC International Nuclear Data Committee*, 2014.

# Appendix

## DESCRIPTION OF THE PROPOSED EXPERIMENT

The experimental setup comprises:

| Part of the | Availability | Design and manufacturing |
|---|---|---|
| COLLAPS | ☒ Existing | ☒ To be used without any modification |

HAZARDS GENERATED BY THE EXPERIMENT:
Hazards named in the document relevant for the fixed COLLAPS installation.

Additional hazards: no additional hazards